Journal of Controlled Release 320 (2020) 96–104

Contents lists available at ScienceDirect

Journal of Controlled Release

journal homepage: www.elsevier.com/locate/jconrel

# Nanostructured toxins for the selective destruction of drug-resistant human CXCR4$^+$ colorectal cancer stem cells

Naroa Serna[a,b,c,*,1], Patricia Álamo[c,1], Prashanthi Ramesh[e,f], Daria Vinokurova[e,f], Laura Sánchez-García[a,b,c], Ugutz Unzueta[c,d], Alberto Gallardo[c,d], María Virtudes Céspedes[c,d], Esther Vázquez[a,b,c], Antonio Villaverde[a,b,c,*], Ramón Mangues[c,d,*], Jan Paul Medema[e,f]

[a] Institut de Biotecnologia i de Biomedicina, Universitat Autònoma de Barcelona, Bellaterra, 08193 Barcelona, Spain
[b] Departament de Genètica i de Microbiologia, Universitat Autònoma de Barcelona, Bellaterra, 08193 Barcelona, Spain
[c] CIBER de Bioingeniería, Biomateriales y Nanomedicina (CIBER-BBN), Bellaterra, 08193 Barcelona, Spain
[d] Biomedical Research Institute Sant Pau (IIB-Sant Pau) and Josep Carreras Research Institute, Hospital de la Santa Creu i Sant Pau, 08025 Barcelona, Spain
[e] Amsterdam UMC, Univ of Amsterdam, LEXOR, Center for Experimental and Molecular Medicine, Cancer Center Amsterdam, Meibergdreef 9, 1105AZ Amsterdam, Netherlands
[f] Oncode Institute, Meibergdreef 9, 1105AZ Amsterdam, Netherlands

ARTICLE INFO

*Keywords:*
Protein nanoparticles
Genetic engineering
Self-assembling
Drug delivery
Cancer stem cells
Cell signaling

ABSTRACT

Current therapies fail to eradicate colorectal Cancer Stem Cells (CSCs). One of the proposed reasons for this failure is the selection, by chemotherapy exposure, of resistant cells responsible for tumor recurrence. In this regard, CXCR4 overexpression in tumor associates with resistance and poor prognosis in colorectal cancer (CRC) patients. In this study, the effectiveness of engineered CXCR4-targeted self-assembling toxin nanoparticles has been explored in the selective killing of CXCR4$^+$ human colon-CSCs compared to 5-Fluorouracil and Oxaliplatin, both classical CRC chemotherapeutic agents. To assess this, 3D spheroid colon-CSCs cultures directly derived from CRC patients and CRC-CSC spheroid-derived tumor mouse models were developed. In these animal models, nanostructured toxins show highly selective induction of pyroptosis in the absence of apoptosis, thus having a great potential to overcome tumor resistance, since the same tumor models show resistance to chemotherapeutics. Results set the basis for further development of more efficient therapies focused on selective CXCR4$^+$ CSCs elimination activating non-apoptotic mechanisms and represent a pre-clinical proof of concept for the use of CSCs-targeted nanostructured toxins as protein drugs for CRC therapy.

## 1. Introduction

Cancer stem cells (CSCs) have been suggested to be the tumorigenic root of cancers due to their clonogenic and high self-renewal capacity [1]. Previous studies have highlighted the potential role of CSCs in tumor recurrence and relapse due to their resistant nature to conventional therapy [2]. The development of treatment strategies that can specifically target and eliminate CSCs are therefore expected to enable long-lasting clinical responses. Nowadays, stage 3 CRC patients are routinely treated with co-adjuvant chemotherapy (5-fluorourocil (5-FU), oxaliplatin and Irinotecan) after radical resection of the primary tumor. However, after a period of remission, cancer recurs in nearly 35% of all cases, possibly because these drugs do not promote complete elimination of colon CSCs. This decreased sensitivity of colon CSCs to the apoptotic stimuli induced by chemotherapeutics is caused by an increased expression of anti-apoptotic proteins, mostly Bcl-xl [3]. Thus, compounds able to overcome these potent anti-apoptotic defenses makes such agents especially valuable for the effective death of colon CSC.

Moreover, a subset of CRC-CSCs that overexpress the chemokine receptor CXCR4 plays a critical role in the poor response to chemotherapy [4]. Consistently, CXCR4 overexpression in CRC tumors increases the risk of recurrence and poor survival [5]. Thus, CXCR4 overexpression in CRC has been associated with the cancer stem cell phenotype and resistance to chemotherapy drugs, such as 5-Fluorouracil [6], in a way similar to other tumor types [7].

In this context, we addressed the urgent need to develop new drugs that can specifically target and kill CXCR4$^+$ CRC-CSCs, which must be

* Corresponding authors at: CIBER de Bioingeniería, Biomateriales y Nanomedicina (CIBER-BBN), Bellaterra, 08193 Barcelona, Spain.
*E-mail address:* naroa.serna@uab.cat (N. Serna).
[1] Equally contributed.

https://doi.org/10.1016/j.jconrel.2020.01.019
Received 7 August 2019; Received in revised form 8 January 2020; Accepted 9 January 2020
Available online 10 January 2020
0168-3659/ © 2020 Published by Elsevier B.V.

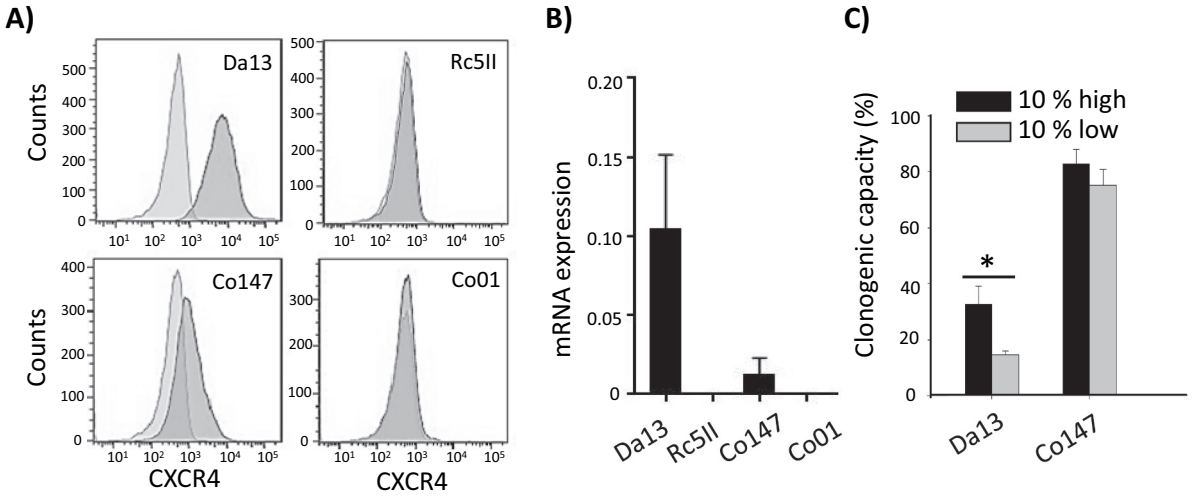



**Fig. 1.** CXCR4 expression in colon CSC cultures. (A) FACS analysis of CXCR4 expression. (B) Expression of CXCR4 evaluated by quantitative RT-PCR, error bars represent s.d. ($n = 2$). (C) Correlation of CXCR4 expression with clonogenic potential. 10% high refers to the 10% of cell population with highest expression of the CXCR4 receptor and 10% low to the 10% of the cell population with lowest expression. Significant differences between relevant data pairs are indicated as * $p < .01$.

necessarily based on new concepts for advanced drug design. To that purpose, we exploited the CXCR4-overexpression occurring in CRC-CSCs to design targeted toxin-based nanoparticles against CXCR4$^+$ CSCs.

The use of nanoparticles as vehicles for targeted drug delivery significantly increases efficiency of the delivery of payload drug to the target cells and mitigates side effects of conventional chemotherapy because of limited biodistribution to normal tissues [8]. The architectonic control of nanoparticle size allows achieving an optimal structure in order to avoid renal clearance [9]. Protein materials are gaining interest in nanomedicine because of the unique combination of regulatable function and structure. Self-assembling protein domains such as cationic stretches offer unique opportunities to generate protein-only nanostructured materials that promote oligomerization of the whole polypeptide [10]. These self-assembling domains can be fused to cytotoxic proteins to generate protein-only, fully stable nanoparticles with intrinsic therapeutic activities [11]. Among cytotoxic peptides, toxins are highly bioactive molecules that inhibit protein synthesis on cells leading to cell death. We have engineered the catalytic domain of the diphtheria toxin (DITOX) and the *Pseudomonas aeruginosa* exotoxin (PE24) as self-assembling therapeutic materials targeted to CXCR4, for the systemic treatment of CXCR4 overexpressing colon cancer tumors. Both microbial toxins are extremely lethal ribosome inactivating proteins (RIPs) that inhibit the eukaryotic elongation factor 2 (eEF-2), impeding protein syntheses and therefore leading to irreversible cell death. When fused to the CXCR4 ligand T22, both form nanoparticles between 30 and 60 nm in size and the repeated systemic administration of both nanostructured drugs in a colorectal cancer xenograft mouse model promotes efficient and specific local destruction of target tumor tissues [12].

As conventional treatments can kill bulk tumor cells but fail to induce durable clinical results likely because they are not effective enough at eliminating CSCs, the cytotoxic effect of toxin-based nanoparticles on colon CSCs should be further explored.

## 2. Results

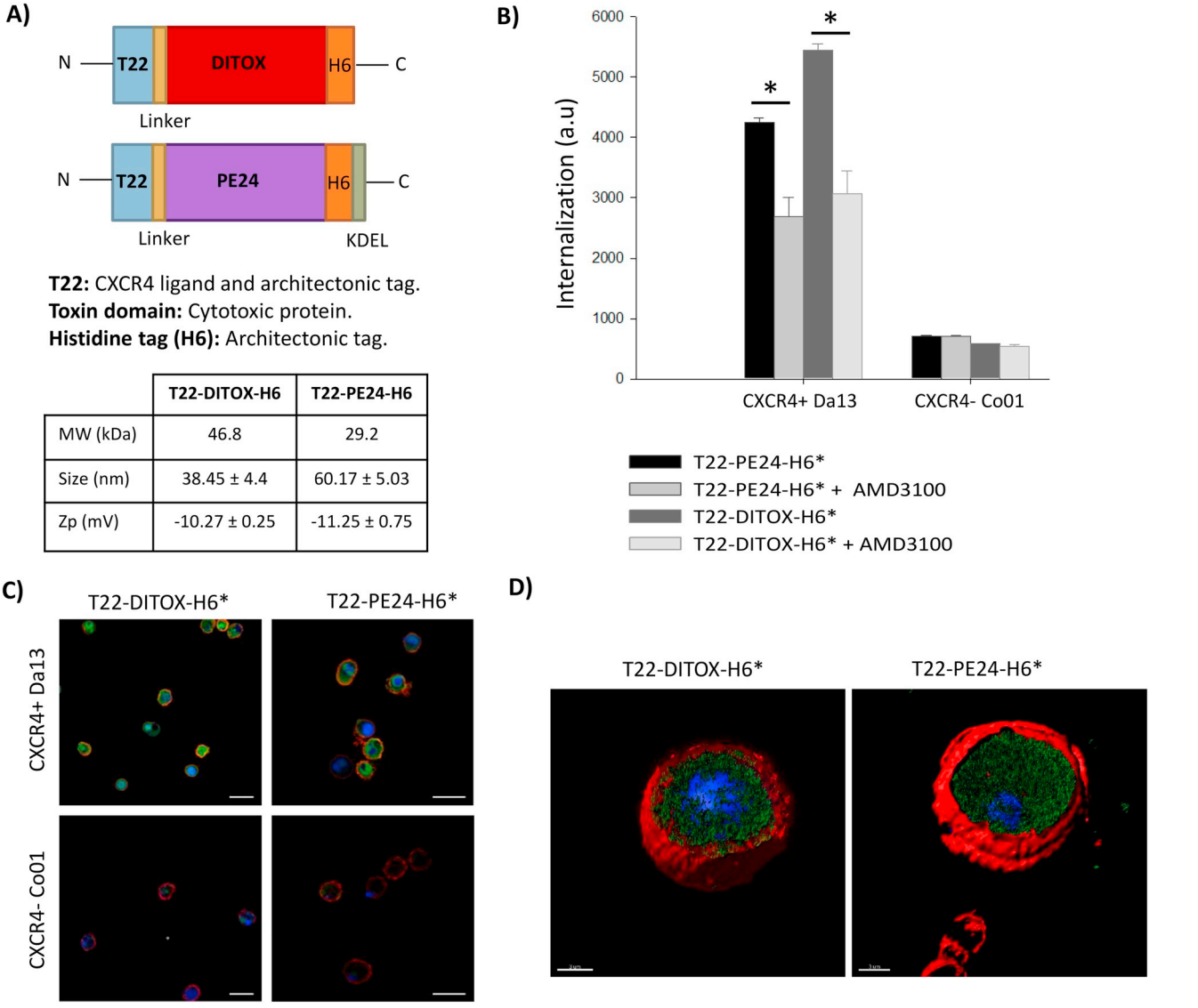
In this study, we have investigated whether CXCR4-targeted self-assembling toxin-based nanoparticles were effective against colon CSCs and could be valuable tools for colon-CSC-specific therapy. For that, we used 3D spheroid colon-CSC cultures directly derived from patients with colorectal cancer and developed CXCR4$^+$ colon CSC mouse model derived from CXCR4$^+$ spheroids.

Tumor spheroids are one of the most versatile scaffold-free methods for three-dimensional (3D) cell culture that have gained increasing interest in drug discovery. These cultures provide highly relevant physiological information regarding cell-cell interactions, hypoxia, drug penetration, response and resistance, being a powerful tool for CSC therapy research [13]. The colon CSCs within colon carcinomas can be propagated in vitro as spheroid cultures retaining tumorigenic capacity under specific conditions. On this basis, we first determined the expression levels of CXCR4 surface marker using flow cytometry in four CRC spheroid cell lines directly derived from patients. Differential CXCR4 expression in CSC cultures was observed with the highest level in Da13 cell line, low expression in Co147 and negative results for RC511 and Co01 cell lines (Fig. 1A). This differential expression was confirmed by RT-PCR (Fig. 1B).

To test the association of CXCR4 marker expression with clonogenicity, we selected the cell lines with CXCR4 expression. CXCR4$^+$ Da13 and CXCR4$^+$ Co147 cells were sorted for population with highest (10% high) and lowest (10% low) expression of the receptor followed by limiting dilution assay to compare clonogenic capacity of these two populations. Limiting dilution analysis shows that the high CXCR4 population in Da13 is more clonogenic compared to the low CXCR4 population (Fig. 1C). However, the results obtained in Co147 (this cell line shows a mild expression of CXCR4) show that this receptor is not a stemness marker in this cell line, probably because CXCR4 expression is not strong enough in Co147 since stemness is associated with high CXCR4 overexpression. These results suggest that CXCR4 is involved in stem cell function in Da13 spheroids (Fig. 1C).

Then, we tested the ability of CXCR4 targeted protein nanoparticles to bind and penetrate, in a receptor-dependent way, CXCR4$^+$ colon CSCs. The assembled T22-DITOX-H6 and T22-PE24-H6 (Fig. 2A), upon labelling with the fluorescent dye ATTO488 (named as T22-DITOX-H6* and T22-PE24-H6* respectively), efficiently entered CXCR4$^+$ Da13 cells but were not efficient internalizing into CXCR4- Co01 cell line. Moreover, the CXCR4-dependent uptake was demonstrated through the inhibition of T22-CXCR4 interaction by AMD3100 that significantly reduced ($p < .01$) the intracellular fluorescence in Da13 cells upon exposure (Fig. 2B). CXCR4 mediated internalization was confirmed by confocal laser microscopy images where labeled nanoparticles were clearly observed as membrane-free entities in the cell cytosol of CXCR4$^+$ cells (Fig. 2C-D). On the other hand, in CXCR4$^-$ Co01 spheroids, nanoparticle uptake was almost negligible, confirming the data obtained by flow cytometry (Fig. 2C).

Once the internalization was evaluated, we explored toxin




| | T22-DITOX-H6 | T22-PE24-H6 |
|---|---|---|
| MW (kDa) | 46.8 | 29.2 |
| Size (nm) | 38.45 ± 4.4 | 60.17 ± 5.03 |
| Zp (mV) | -10.27 ± 0.25 | -11.25 ± 0.75 |

**Fig. 2.** Protein nanoparticles and CXCR4 specific internalization in CSC spheroid cultures. (A) Schematic representation of the polypeptidic building blocks of toxin nanoparticles used in the study. Box sizes are only indicative. Relevant properties of the nanoparticles are shown in the table at the bottom. Details of the aa sequences and nanoparticle characterization can be found elsewhere (Sanchez-Garcia et al., 2018). (B) Internalization of 100 nM of T22-DITOX-H6* and T22-PE24-H6* upon 2 h of exposure and uptake inhibition by AMD3100 in spheroid cultures. (C) Confocal microscopy of cultured Da13 and Co01 single cells exposed to 100 nM of ATTO488-labeled toxin nanoparticles showing their intracellular localization. Bars indicate 20 μm. (D) 3D image reconstructions of confocal stacks obtained of Da13 single cells upon exposure to T22-DITOX-H6* and T22-PE24-H6* nanoparticles. Bars indicate 3 μm. Blue label corresponds to the nucleus part, red label to cell membranes and green to the nanoparticles. All images were taken 2 h after exposure. Nanoparticles are located inside the cell between nuclear membrane (the top of the nucleus) and cell membrane. Significant differences between relevant data pairs are indicated as * $p < .01$. MW: Molecular weight. Zp: Zeta potential. (For interpretation of the references to colour in this figure legend, the reader is referred to the web version of this article.)

nanoparticle mediated cytotoxicity in CXCR4$^+$ Da13 cell line, showing an IC50 of 0.15 μM and 0.06 μM for T22-PE24-H6 and T22-DITOX-H6 respectively (Fig. 3A). Cytotoxicity was clearly detectable in CXCR4$^+$ Da13 cell line but it was abolished ($p < .01$) upon treatment with AMD3100. In addition, toxicity was not observed in the CXCR4$^-$ Co01 cell line, which indicates specific cell death mediated by CXCR4 binding (Fig. 3B). Because of the potent cytotoxic activities of both proteins, we also checked cell viability in human colon organoids that were derived from normal colon tissue and cultured in matrigel. First, we analyzed the CXCR4 expression in these cells. As expected, normal colon cells did not express the receptor (Fig. 3C, inset). More interestingly, toxicity was not detected in cells treated with functional nanoparticles (Fig. 3C).

Due to the higher cytotoxicity of T22-DITOX-H6 in comparison to T22-PE24-H6 (Fig. 3A), we selected this nanoparticle for the following experiments. When CXCR4$^+$ Da13 spheroid cultures were treated with Oxaliplatin and 5-FU chemotherapeutic compounds and nanoparticles at equimolar concentration (1 μM), we observed a strong initial decrease in cell viability in the first 2 days for all treatments. However, when we measured the growth of the cultures over time (up to 8 days), we detected that cells treated with either 5-Fluorouracil or oxaliplatin regained proliferative potential, suggesting that clonogenic colon CSCs survived the therapy. In contrast, treatment with T22-DITOX-H6 inhibited this revival strongly (Fig. 3D). Importantly, at 100 nM, at which only receptor mediated cytotoxicity of the nanoparticles was demonstrated (Fig. 3B), T22-DITOX-H6 remained more effective than the other drugs (Fig. 3D). This indicates that targeting CXCR4$^+$ CSCs with toxin protein fusions is a promising approach for colon-CSC therapy. This resulted probably due to the combined effect of CXCR4$^+$ cancer stem cell targeting and potent cytotoxicity of toxins.

Due to the highly specific cytotoxicity observed by the T22-DITOX-

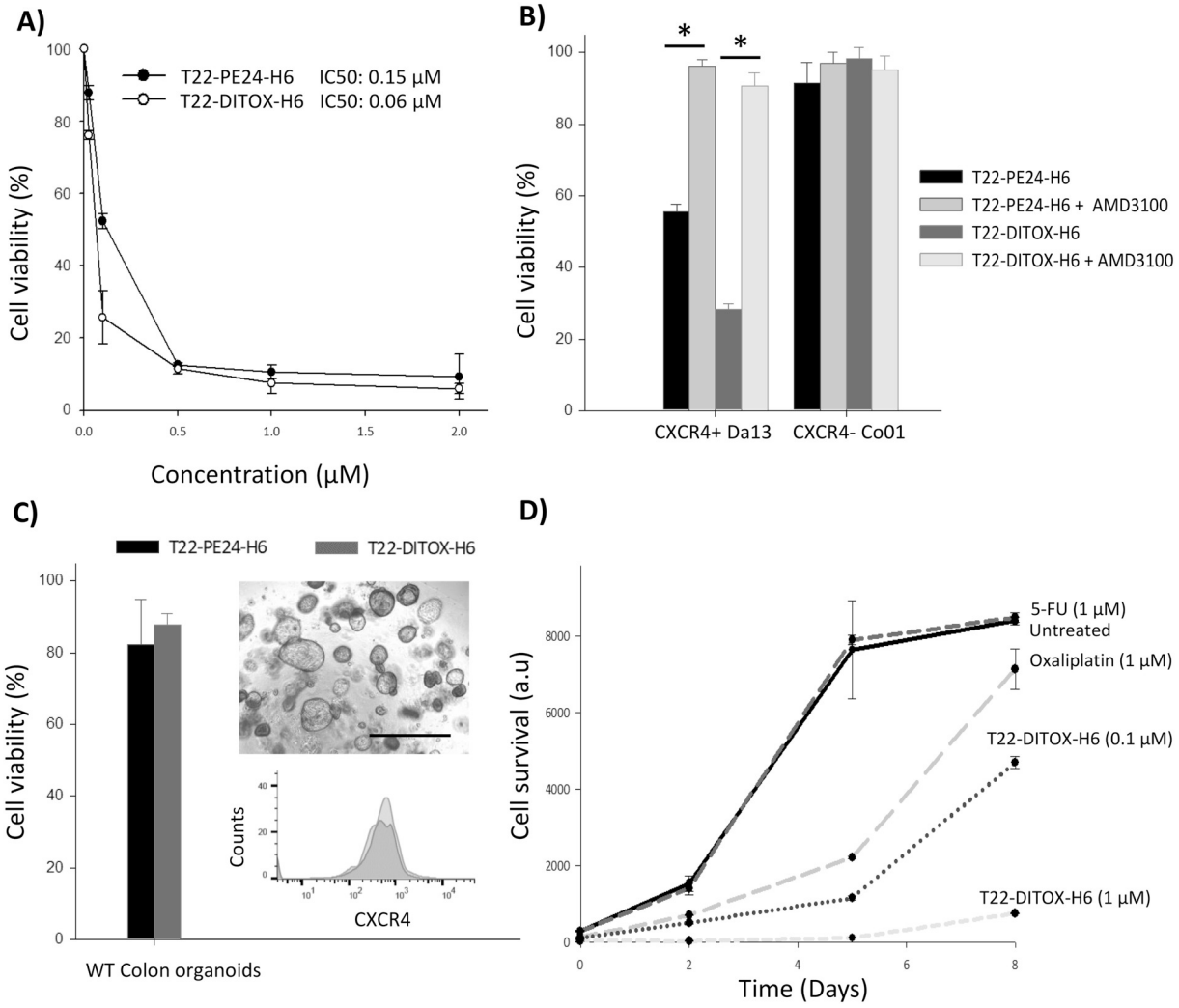



**Fig. 3.** Cytotoxicity and cell survival of CSC spheroids upon nanoparticle treatment. (A) Cell death induced by T22-DITOX-H6 and T22-PE24-H6 at different concentrations over CXCR4$^+$ Da13 spheroids 48 h after exposure. (B) Comparison of cell death induced by 100 nM of toxin-based nanoparticles in CXCR4$^+$ and CXCR4$^-$ colon CSCs spheroids and inhibition of Da13 cell death by the CXCR4 antagonist AMD3100 (C) Cell viability in normal human colon organoids upon treatment with 100 nM of toxin-based nanoparticles 48 h after exposure. In the inset, light microscope image of human colon organoids isolated from a healthy section of resected colon segment derived from a patient and fluorescence-activated cell sorting analysis of CXCR4 expression. Organoids cultured in matrigel show a cystic morphology of epithelial cells growing spherically with a lumen in the middle (image taken at 4×; scale bars indicate 1000 μm). (D) Cell survival upon treatment with equimolar concentrations of T22-DITOX-H6 and chemotherapeutics over Da13 spheroid cultures at various time points. Significant differences between relevant data pairs are indicated as * $p < .01$.

H6 nanoparticle in CXCR4$^+$ CSC spheroid cell cultures, we next tested the tolerability and the effect of this targeted toxin in in vivo CSC spheroid-derived mouse models. For this, we evaluated the specificity, antitumor activity and toxicity of T22-DITOX-H6. We i.v. administered 30 μg of T22-DITOX-H6 at 5, 24 and 48 h in two subcutaneous colorectal cancer spheroid-derived models; one model derived from CXCR4 high Da13 spheroids and the second one displaying no CXCR4 expression (Co01). After a single dose i.v. injection the number of cell death bodies in the CXCR4$^+$ CRC-CSC (Da13) subcutaneous tumors was significantly higher ($p < .001$) than in the CXCR4$^-$ CRC-CSC (Co01) tumors in the studied time range (5, 24 and 48 h) (Fig. 4). We observed a significant increase ($p < .001$) in the number of death cells in CXCR4$^+$ Da13 tumors at 48 h after nanoparticle injection in comparison with 24 h and 5 h, as well as at 24 h versus 5 h (Fig. 4).

Additionally, significant differences were observed in the number of mitotic figures and proliferation index in Da13 tumors, measured by ki67 staining. These tumors showed a significant reduction in both the number of mitotic figures at 48 h compared to 24 h or 5 h ($p < .000$). In the same way, a significant decrease was observed in mitotic figure count at 24 h when compared to 5 h ($p < .000$) (Fig. 5).

To analyze whether T22-DITOX-H6 treatment selectively killed CXCR4$^+$ cancer cells as well as the mechanism of cytotoxicity we administered a single i.v. bolus of this nanoparticle in CXCR4$^+$ CRC-CSC (Da13) mouse model. We evaluated the expression of CXCR4 in tumor tissue along time and the activation of proteins involved in apoptosis and pyroptosis between the control and treated tumors by immunohistochemistry.

Interestingly, T22-DITOX-H6 treated tumors showed an increase of CXCR4 expression in tumor tissue at 24 h and 48 h as compared to buffer-treated animals (Fig. 6A). Regarding the mechanism of cytotoxicity of T22-DITOX-H6, there was no detectable immunostaining when applying IHC against apoptotic markers, cleaved Caspase3 and PARP proteolysis, in Da13 T22-DITOX-treated tumors, suggesting than the mechanism of cell death was not mediated by apoptosis induction. However, DNA damage marker measured by H2X gamma IHC, showed a trend toward higher expression in Da13 tumors at 48 h vs 24 h and 5 h tumors (Fig. 6B). Besides apoptosis, there are other cell death mechanisms playing widespread physiopathological roles with therapeutic

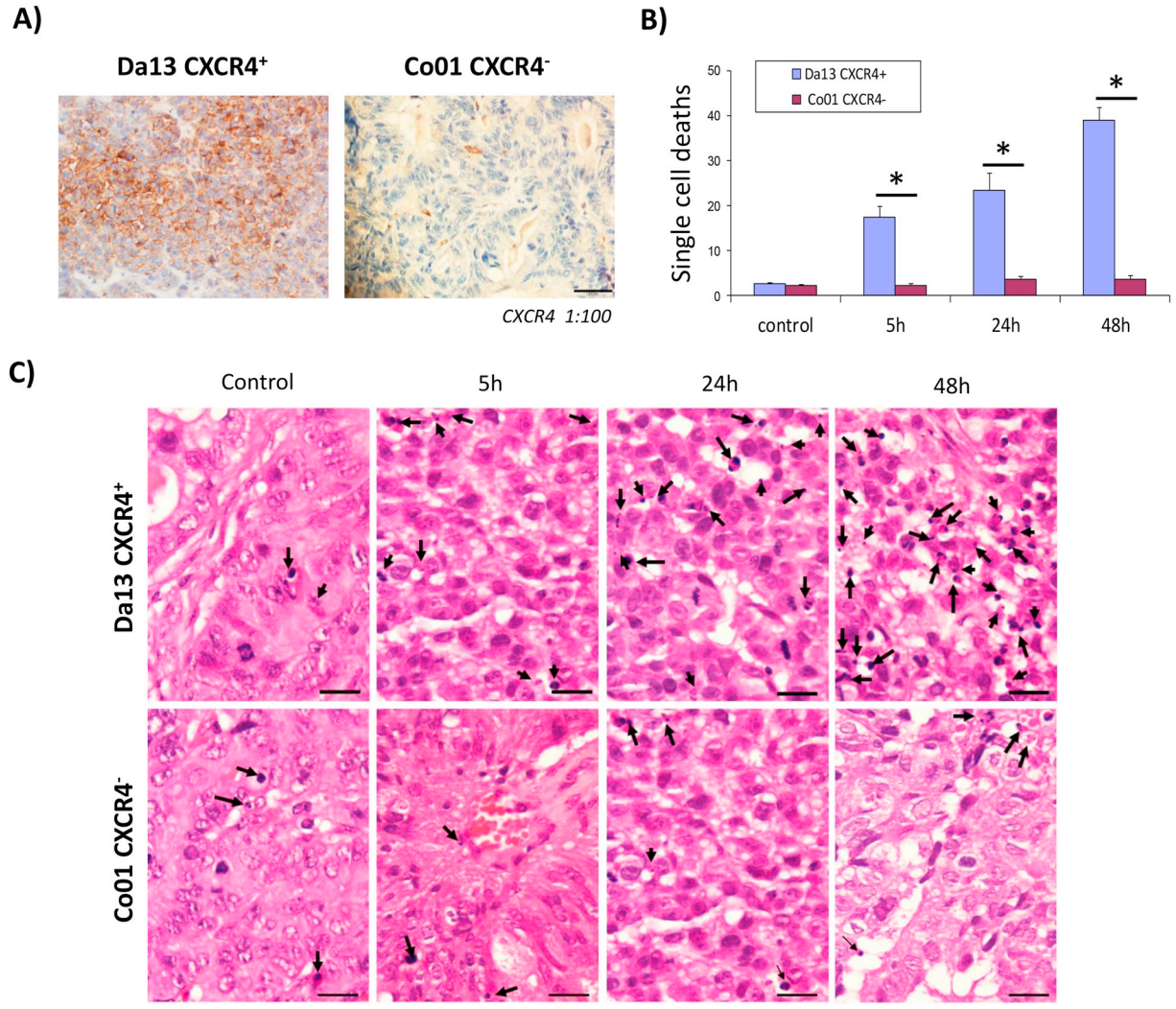



**Fig. 4.** Induction of cell death after T22-DITOX-H6 nanoparticle injection in subcutaneous CRC-CSC tumors derived from CXCR4$^+$ or CXCR4$^-$ organoids. (A) Representative immunohistochemical CXCR4 staining of CXCR4$^+$ Da13 and CXCR4$^+$ Co01 organoid-derived subcutaneous tumors. Bar: 50 μm. (B) Cell death bodies in H&E tumor slices per ten high-power fields (400× magnification) are plotted at different time points (5, 24 and 48 h) after single bolus injection of 30 μg of T22-DITOX-H6. (C) Representative H&E staining of subcutaneous tumors showing cell deaths (black arrows). Bar: 20 μm. Statistical significance *$p < .001$. H&E: Hematoxylin and eosin stain.

implications. Similar to apoptosis, pyroptosis, which is an inflammatory caspase-dependent form of programmed cell death that occurs usually in response to microbial infection, promotes nuclear condensation and chromatin DNA fragmentation in pyroptotic cells. Surprisingly, pyroptosis markers Caspase 11 and NLPR3 showed a higher expression in Da13 tumors at 48 h vs 24 h and 5 h tumors, indicating that T22-DITOX-H6 induces pyroptosis in colon-CSCs (Fig. 6C).

In a step further, we assessed the antitumor effect of T22-DITOX-H6 compared to 5-FU in a CXCR4$^+$ subcutaneous CRC-CSC mouse model after repeated dose administration. After a dosage schedule of equimolar concentration of T22-DITOX-H6 and 5-FU (10 μg and 1.5 mg/kg respectively), every 2 days, per 6 doses, mice were analyzed. Toxin-treated group displayed a greater inhibition of tumor growth compared with chemotherapy and untreated control group at the end of the experiment (Fig. 7A), supporting the higher T22-DITOX-H6 effectiveness over 5-FU killing CXCR4$^+$ CRC-CSCs. Moreover, no significant differences in body weight between experimental and control groups were observed (Fig. 7B) with no toxicity in normal tissues (Fig. 7C).

## 3. Discussion

There are no available effective colon CSC-targeted therapies that are active in tumors showing resistant to classical drugs. Therefore, it is important to develop new treatments able to target and efficiently kill this chemotherapy-refractory population in colon tumors. As CSCs are less primed to mitochondrial death due to an enhanced anti-apoptotic threshold, one of the main strategies in CRC therapy is based in the use of anti-apoptotic inhibitors such as BH3 mimetics to sensitize colon CSCs toward chemotherapy. However, the heterogeneity of tumors with respect to their sensitivity to various death stimuli, further emphasizes the need for alternative death pathways in the therapeutic control of cell death.

We demonstrated that targeted nanotoxins effectively kill highly clonogenic CXCR4$^+$ cultured spheroids, in a receptor-dependent way, and that also limit the growth of tumors derived from CXCR4$^+$ spheroids, while the same in vitro and in vivo tumor models show resistance to equimolar concentrations of 5-FU. In this regard, it is important to

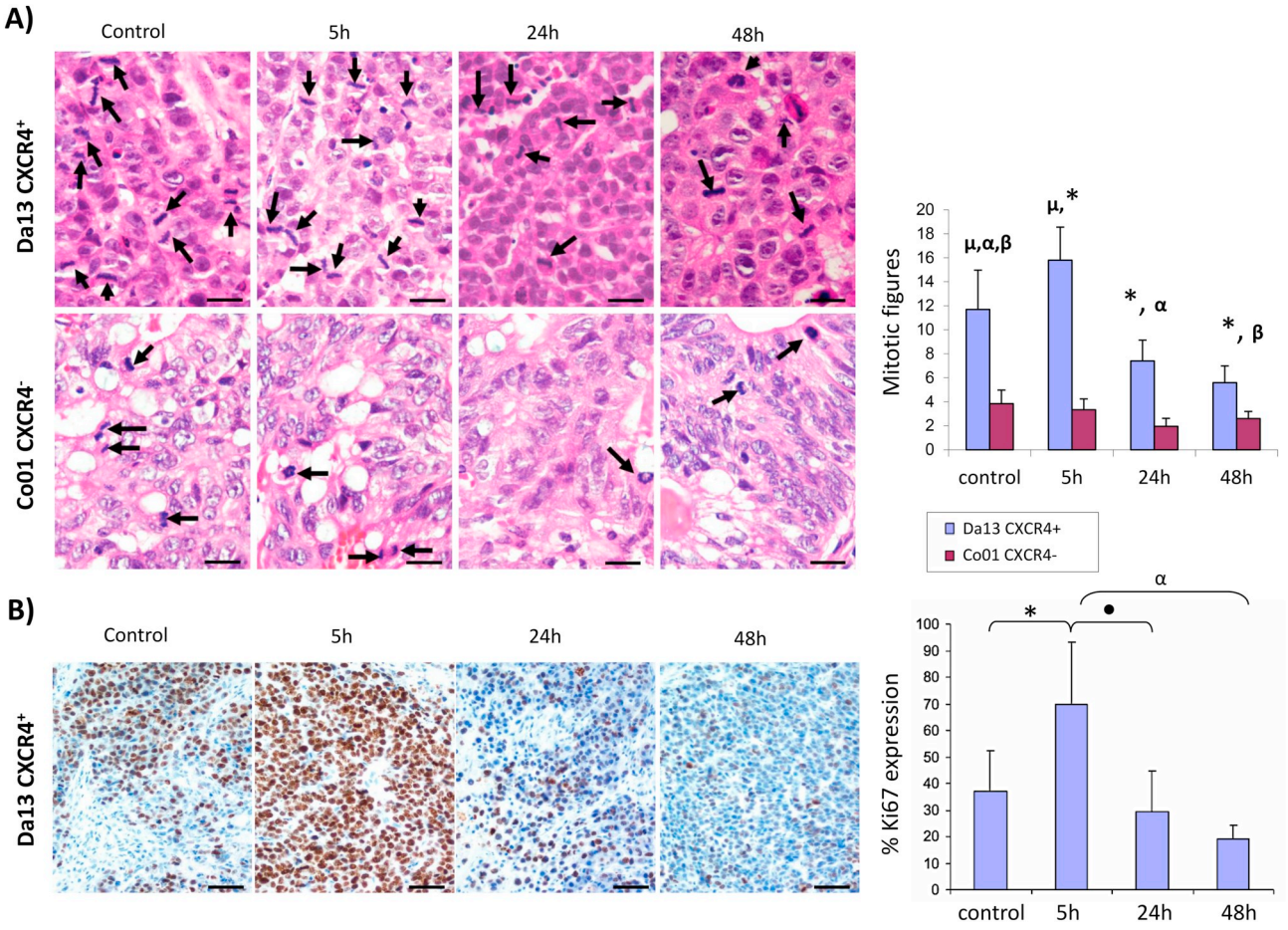



**Fig. 5.** Proliferative deregulation after T22-DITOX-H6 nanoparticle injection in subcutaneous tumors derived from CXCR4$^+$ and CXCR4$^-$ CRC-CSC organoids. (A) Representative H&E staining of CXCR4$^+$ and CXCR4$^-$ CRC organoid subcutaneous tumors showing mitotic figures at 5 h post-treatment (black arrows). Bar: 20 μm. Quantification of the number of mitotic cell figures in H&E tumor slices per ten high-power fields (400× magnification) are plotted for each time studied. Statistical significance: $^{\mu}p = 0.02$, $^{*}p < .000$, $^{\beta}p = 0.037$, $^{\alpha}p = 0.002$. H&E: Hematoxylin and eosin stain. (B) High Ki67 expression displaying high tumor cell proliferation 5 h after T22-DITOX-H6 (30 μg single dose) nanoparticle injection in subcutaneous CRC-CSC tumors derived from CXCR4$^+$ organoids, whereas a progressive proliferation block occurs during the 24-48 h post-treatment period (low mitotic number and negligible Ki67 expression). Statistical significance: $^{*}p = .025$, $^{\bullet}p = .033$, $^{\alpha}p = 0.021$.

remark that a likely reason for T22-DITOX-H6 to control tumor growth, when given at a repeated-dose schedule, is the use of a dosage interval (here every 48 h) that administers the dose at the peak of CXCR4 tumor expression; thus, enhancing its effect on target cancer cells, while avoiding its distribution and damage over normal cells. We have observed a similar increase in CXCR4 tumor expression 48 h after the administration of a drug-nanoparticle conjugate, which also blocked tumor growth using a 2 day interval for injection of repeated doses leading to a significantly reduced CXCR4$^+$ cancer cell fraction at the end of treatment [14]. This effect could be due to the plasticity of cancer cells that can dedifferentiate to generate new CXCR4$^+$ CSC to replenish the selectively killed CXCR4$^+$ CSC in the tumor. However, after multiple doses differentiated cells in the tumor may lose progressively their capacity to dedifferentiate to generate fewer additional CXCR4$^+$ CSC with each subsequent dose.

Previous reports indicate that CRC cells become resistant to chronic exposure to 5-fluorouracil through the emergence of a cancer cell population that express stem cell markers, including CXCR4 [15]. Similarly, oxaliplatin-resistant colorectal cancer cells show CXCR4 overexpression and activation of its signaling pathway related to chemotaxis, cell survival and/or proliferation [16]. Indeed, acquired resistance to chemotherapy occurs through the recruitment of new genetic mutations or epigenetic changes in cancer cells. It causes an increase in the activity of signaling pathways that block apoptosis and/or increase proliferation, thus leading to tumor outgrowth [17]. Because of the acquisition of an aggressive phenotype, resistant tumors in patients grow faster than the naïve untreated tumor [18]. According with this, our data also support the notion that tumors treated with 5-FU could have incorporated new mutations that induce tumor outgrowth, as compared with untreated tumor controls.

We have here developed T22-DITOX-H6 as a targeted nanomedicine approach that is effective against CXCR4$^+$ CRC stem cells that have shown poor response to 5-FU or oxaliplatin both in vitro and in vivo. We envisage two main reasons underlying the higher effectiveness of T22-DITOX-H6 eliminating CSCs:

1) The highly selective delivery of the therapeutic moiety made possible because of the design of a nanoparticle with appropriate pharmacokinetics (size higher than renal filtration cut-off) and the incorporation of a highly specific ligand that selectively binds the

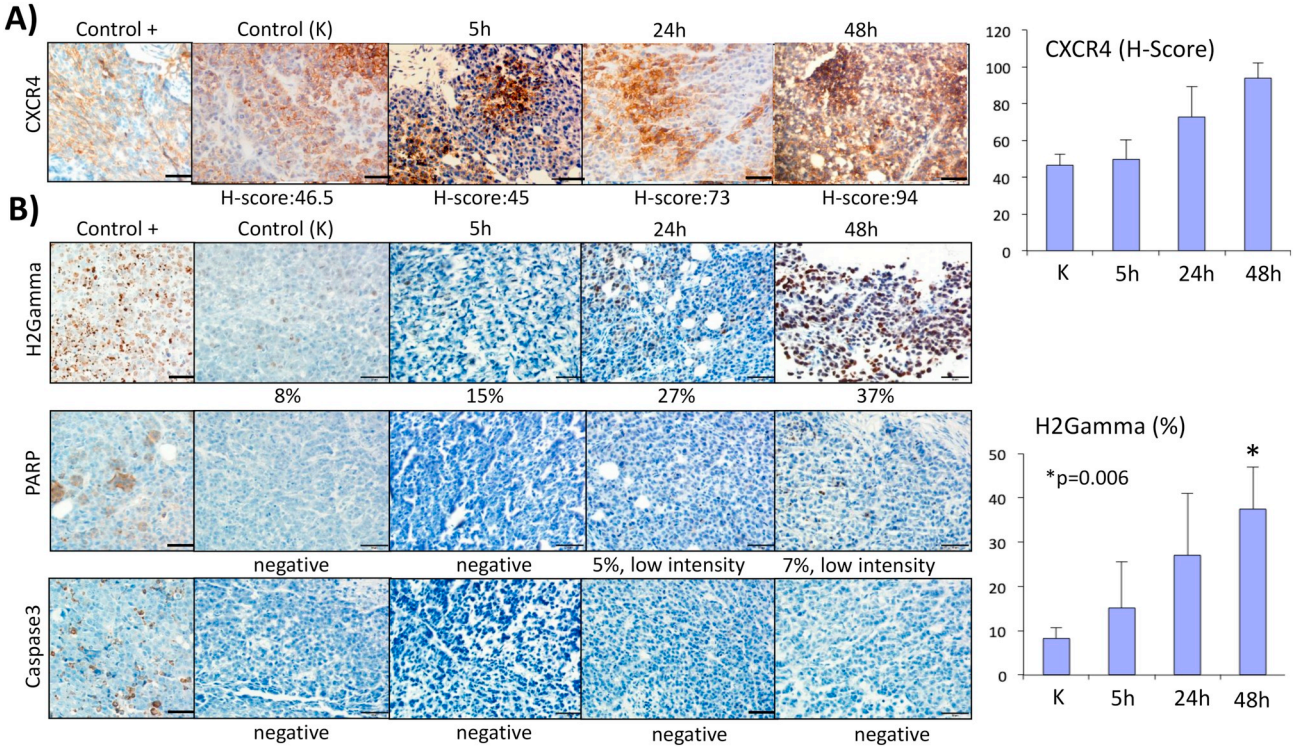



**Fig. 6.** CXCR4 expression and cell death mechanism in Da13 tumors treated with T22-DITOX-H6. (A) Representative pictures of IHC staining of CXCR4 expression in tumors at 5, 24 or 48 h after injection of 30 μg of T22-DITOX-H6. (B) Immunostaining of apoptotic markers: Caspase3, PARP proteolysis and H2AX gamma staining at 5, 24 or 48 h in Da13 subcutaneous tumors. (C) Immunostaining of pyroptosis markers: Caspase 11 and NLPR3 expression along time in Da13 tumors, showing activation of these two pyroptotic mediators especially 48 h post-therapy. Original magnification: 400 x. IHC: Immunohistochemical staining.

CXCR4 receptor and the high overexpression of CXCR4 in cancer cells as compared to normal cells. This allows the specific delivery of the toxin to CXCR4$^+$ target cancer cells without significant exposure to normal tissue. Without receptor, targeting the nanoparticle could not be directly administered to the animals because of severe toxicity.

2) The capacity of the toxins, and specifically the diphtheria toxin of triggering a cell death mechanism mutually exclusive with apoptosis. T22-DITOX-H6 kills cells by binding to a CXCR4 receptor, internalizing via a coated pit, translocating its active fragment into the cytosol, and enzymatically ADP-ribosylating elongation factor-2. This in turn inhibits protein synthesis and cells die by diverse mechanisms. Thus, depending on the context, bacterial exotoxins induces necroptosis [19] or other non-apoptotic cell death mechanisms, such as pyroptosis [20], which activate pathways that differ from those mediating apoptotic induction [21]. Here, we are describing a high activation of the mediators of pyroptosis Caspase 11 and NLRP3, 48 h after T22-DITOX-H6 treatment in CXCR4$^+$ colon cancer stem cells, in a mouse model, in the absence of activation of apoptotic markers, a time at which tumor cell proliferation is blocked. Indeed, pyroptostic cell death associates with G2/M arrest and according with this [22], our results show that 5 h after T22-DITOX-H6 treatment tumor cells are proliferating (Ki67 highly expressed and mitotic figures observed) whereas at 24 -48 h post-treatment, their stop dividing (Ki67 expression is negligible and lower than vehicle-treated tumors). This proliferative arrest occurs when pyroptosis is induced having their peak at 48 h post-nanotoxin treatment. Therefore, this therapeutic approach can effectively overcome the block in apoptotic induction associated with chemotherapy-resistant tumors [23] by activating pyroptosis as a non-apoptotic and alternative cell death pathway in tumor cells. To our knowledge, this finding represents the first description of pyroptotic cell death by Diphtheria exotoxin in cancer.

## 4. Conclusion

Results obtained here show that CXCR4-targeted toxin nanoparticles target and effectively kill apoptotic-resistant tumors derived from CXCR4$^+$ colon CSCs by triggering pyroptotic cell death. Thus, the use of multi-pathway targeted agents to eradicate colon cancer seems to be an emerging and powerful strategy in CRC-CSC therapy.

In conclusion, toxin-based protein-only nanoparticles are presented as especially valuable tools for the treatment of colon cancer overcoming issues of improve therapeutic efficacy, drug resistance and metastasis. In addition to colorectal cancer [1b], at least 23 additional human tumor types, CXCR4 overexpression associates with the stemness phenotype, therapeutic resistance and shorter time to relapse. Treating all these tumors could also benefit from a therapeutic approach using CXCR4-targeted nanotoxins aimed to selectively eliminate cancer stem cells through pyroptotic induction.

## Acknowledgements

This work was supported by Agencia Estatal de Investigación (AEI), Fondo Europeo de Desarrollo Regional (FEDER, grant BIO2016-76063-R, AEI/FEDER, UE FEDER, ISCSII, PI15/00378 and PIE15/00028), AGAUR (2014SGR-132, 2017 SGR 865 GRC), La Caixa Foundation, and CIBER-BBN Nanomets and Nanoprother Intramural Projects, and

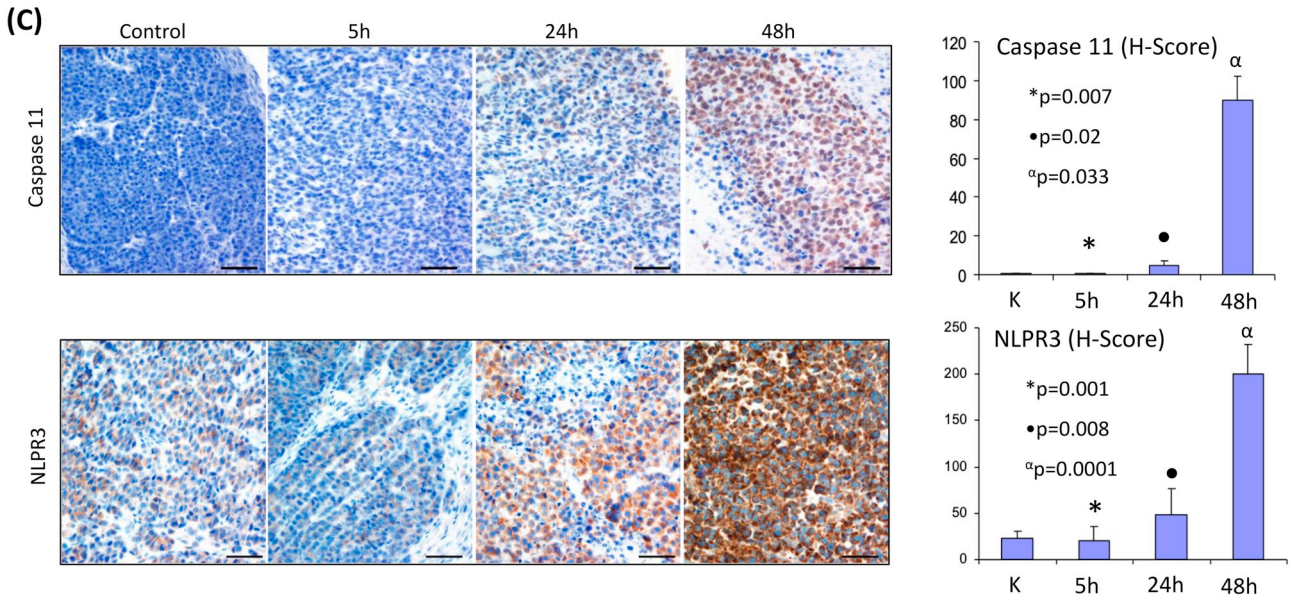



**Fig. 6.** (*continued*)

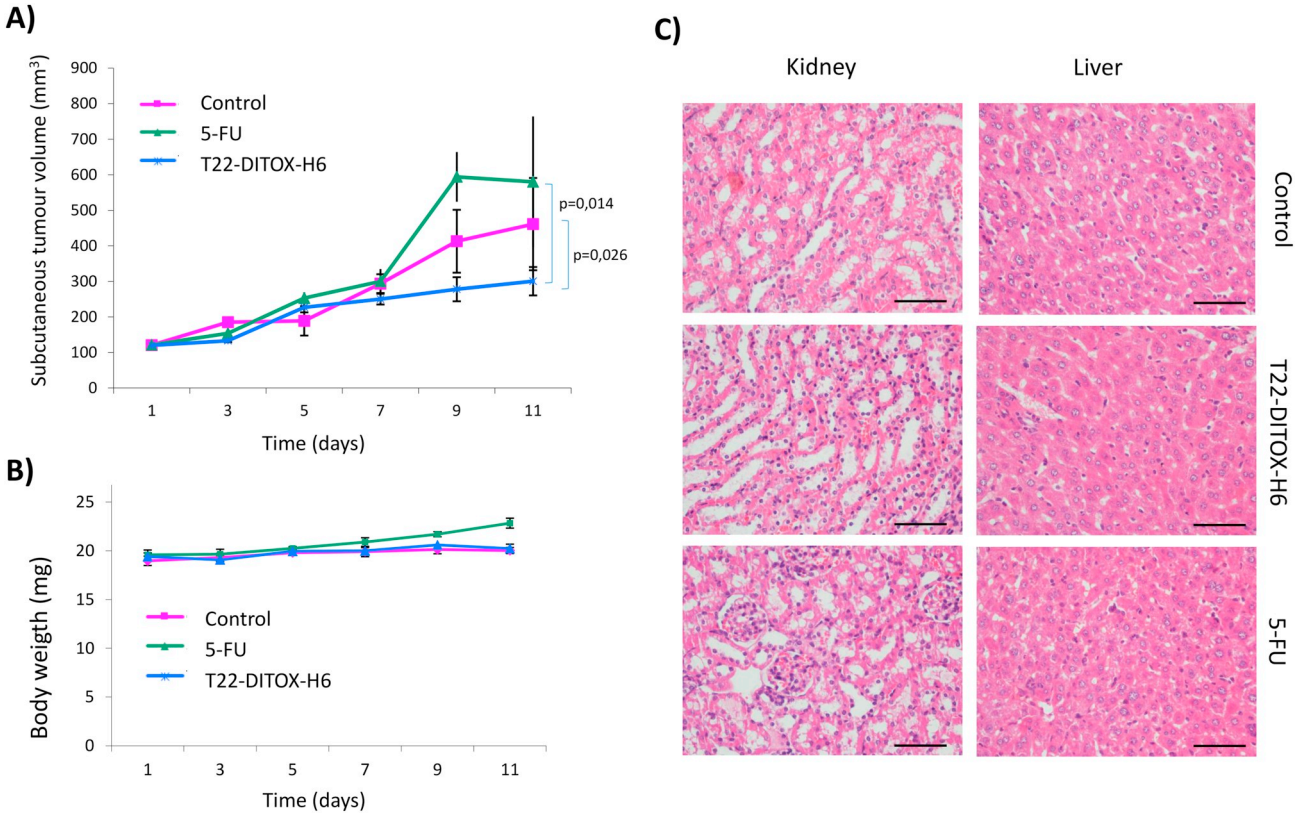



**Fig. 7.** Evaluation of antitumoral effect of T22-DITOX-H6 compared to 5-FU in a CXCR4$^+$ subcutaneous tumor CRC-CSC model derived from organoids after repeated dose administration. (A) Antitumor effect of T22-DITOX-H6 (10 μg) compared to a equimolar dose of 5-FU (1.5 mg/kg), measured by tumor volume at the end of the experiment after repeated dose administration, every 2 days for 6 doses. (B) Evolution of mouse body weight after the described repeated dose regime for the protein nanoparticle and for 5-FU. (C) Representative H&E staining of liver and kidney from control, T22-DITOX-H6 and 5-FU groups showing the absence of histological alterations at the end of the experiment. Bar: 50 μm. H&E: Hematoxylin and eosin stain. All data are presented as mean ± SEM, $n = 7$.

Protein production was partially performed by the ICTS “NANBIOSIS,” more specifically by the CIBER-BBN Nanotoxicology and Protein Production Platform of CIBER in Bioengineering, Biomaterials & Nanomedicine (CIBER-BBN)/IBB, at the UAB sePBioEs scientific-technical service (http://www.nanbiosis.es/portfolio/u1-protein-production-platform-ppp/). We are also indebted to SCAC (UAB) for cell culture facilities and assistance. N·S. was supported by a predoctoral fellowship from the Government of Navarra and EMBO short term fellowship. P.A. obtained a Fellowship from the Josep Carreras Research Institute. L.S.G. was supported by AGAUR (2017FI_B100063). M.V.C. and U.U. are supported by Miguel Servet and Sara Borrell contracts from ISCIII, respectively. A.V. received an ICREA ACADEMIA Award. N.S and P.A contributed equally to this work. MVC, UU, EV and AV are co-inventors in a patent on the uses of T22 as a tumor-targeting agent (WO2012095527). All the in vivo procedures were approved by the Hospital de Sant Pau Animal Ethics Committee and performed according to European Council directives (CEA-OH/9721/2).

## Appendix A. Supplementary data

Supplementary data to this article can be found online at https://doi.org/10.1016/j.jconrel.2020.01.019.

## References

[1] a) J.C. Chang, Medicine (Baltimore) 95 (2016) S20;
b) J. Kim, H. Takeuchi, S.T. Lam, R.R. Turner, H.J. Wang, C. Kuo, L. Foshag, A.J. Bilchik, D.S. Hoon, J. Clin. Oncol. 23 (2005) 2744;
c) N.K. Lytle, A.G. Barber, T. Reya, Nat. Rev. Cancer 18 (2018) 669.
[2] Z. Kozovska, V. Gabrisova, L. Kucerova, Biomed. Pharmacother. 68 (2014) 911.
[3] S. Colak, C.D. Zimberlin, E. Fessler, L. Hogdal, P.R. Prasetyanti, C.M. Grandela, A. Letai, J.P. Medema, Cell Death Differ. 21 (2014) 1170.
[4] a) J.A. Burger, T.J. Kipps, Blood 107 (2006) 1761;
b) A.K. Croker, A.L. Allan, J. Cell. Mol. Med. 12 (2008) 374.
[5] Y.J. Choi, W.J. Chang, S.W. Shin, K.H. Park, S.T. Kim, Y.H. Kim, Onco. Targets. 9 (2016) 3307.
[6] a) A.F. Dessein, M. Fontaine, B.S. Andresen, N. Gregersen, M. Brivet, D. Rabier, S. Napuri-Gouel, D. Dobbelaere, K. Mention-Mulliez, A. Martin-Ponthieu, Orphanet J. Rare Dis. 5 (2010) 26;
b) Y. Touil, W. Igoudjil, M. Corvaisier, A.F. Dessein, J. Vandomme, D. Monte, L. Stechly, N. Skrypek, C. Langlois, G. Grard, Clin. Cancer Res. (2014) 837–846.
[7] D.G. Duda, S.V. Kozin, N.D. Kirkpatrick, L. Xu, D. Fukumura, R.K. Jain, Clin. Cancer Res. 8 (2011) 2074–2080.
[8] M.S. Lee, E.C. Dees, A.Z. Wang, Oncology 31 (2017) 198.
[9] J. Shen, J. Wolfram, M. Ferrari, H. Shen, Mater. Today 20 (2017) 95.
[10] U. Unzueta, N. Ferrer-Miralles, J. Cedano, X. Zikung, M. Pesarrodona, P. Saccardo, E. Garcia-Fruitos, J. Domingo-Espin, P. Kumar, K.C. Gupta, R. Mangues, A. Villaverde, E. Vazquez, Biomaterials 33 (2012) 8714.
[11] N. Serna, L. Sanchez-Garcia, U. Unzueta, R. Diaz, E. Vazquez, R. Mangues, A. Villaverde, Trends Biotechnol. 36 (2018) 318.
[12] L. Sanchez-Garcia, N. Serna, P. Alamo, R. Sala, M.V. Cespedes, M. Roldan, A. Sanchez-Chardi, U. Unzueta, I. Casanova, R. Mangues, E. Vazquez, A. Villaverde, J. Control. Release 274 (2018) 81.
[13] B.W. Huang, J.Q. Gao, J. Control. Release 270 (2018) 246.
[14] M.V. Cespedes, U. Unzueta, A. Avino, A. Gallardo, P. Alamo, R. Sala, A. Sanchez-Chardi, I. Casanova, M.A. Mangues, A. Lopez-Pousa, R. Eritja, A. Villaverde, E. Vazquez, R. Mangues, EMBO Mol. Med. 10 (2018).
[15] Y. Touil, W. Igoudjil, M. Corvaisier, A.F. Dessein, J. Vandomme, D. Monte, L. Stechly, N. Skrypek, C. Langlois, G. Grard, G. Millet, E. Leteurtre, P. Dumont, S. Truant, F.R. Pruvot, M. Hebbar, F. Fan, L.M. Ellis, P. Formstecher, I. Van Seuningen, C. Gespach, R. Polakowska, G. Huet, Clin. Cancer Res. 20 (2014) 837.
[16] W.S. Huang, M.C. Hsieh, C.Y. Huang, Y.H. Kuo, S.Y. Tung, C.H. Shen, Y.Y. Hsieh, C.C. Teng, K.F. Lee, T.C. Chen, K.C. Lee, H.C. Kuo, PLoS One 11 (2016) e0159927.
[17] W. Xuan, Z. Haiyun, C. Xiaozhuo, Cancer Drug Resist 2 (2019) 141–160.
[18] a) S. Sorscher, M. Goodman, S. Ramkissoon, JCO precision, Oncology 2 (2018) 1–4;
b) J.B. Post, N. Hami, Mertens AEE, S. Elfrink, J.L. Bos, Snippert HJG, Oncotarget 14 (2019) 1440–1457.
[19] a) H. Horita, A.E. Frankel, A. Thorburn, PLoS One 3 (2008) e3909;
b) S. Fulda, Cancer Biol. Therapy 14 (2013) 999.
[20] a) S.W. Tait, G. Ichim, D.R. Green, J. Cell Sci. 127 (2014) 2135;
b) K. Nagarajan, K. Soundarapandian, R.F. Thorne, D. Li, D. Li, Transl. Oncol. 7 (2019) 925–931;
c) Y.Y. Wang, X.L. Liu, R. Zhao, Front. Oncol. 9 (2019) 971.
[21] a) L. Steinhart, K. Belz, S. Fulda, Cell Death Dis. 4 (2013) e802;
b) M.B. Meng, H.H. Wang, Y.L. Cui, Z.Q. Wu, Y.Y. Shi, N.G. Zaorsky, L. Deng, Z.Y. Yuan, Y. Lu, P. Wang, Oncotarget 7 (2016) 57391.
[22] a) J.A. Pezuk, EBioMedicine 41 (2019) 17–18;
b) L. Chen, Y. Zhao, D. Lai, P. Zhang, Y. Yang, Y. Li, K. Fei, G. Jiang, J. Fan, Cell Death Dis. 22 (6) (2018) 597.
[23] P. Bouwman, J. Jonkers, Nat. Rev. Cancer 9 (2012) 587–598.